Semicond. Sci. Technol. **11** (1996) 1512–1515. Printed in the UK

Photon-assisted tunnelling through a quantum dot

T H Oosterkamp, L P Kouwenhoven, A E A Koolen, N C van der Vaart and C J P M Harmans

Department of Applied Physics, Delft University of Technology, PO Box 5046, 2600 GA Delft, The Netherlands

Abstract. We report photon-assisted tunnelling (PAT) through a quantum dot with zero-dimensional (0D) states. PAT allows electrons to reach previously inaccessible energy states by absorbing or emitting photons from a microwave signal. We discuss a model based on a master equation for a quantum dot with 0D states and include PAT processes. Simulations are compared with measurements.

1. Introduction

Transport through a quantum dot is regulated by Coulomb blockade effects. The energy to put an extra electron on a quantum dot includes a charging energy E_c and a finite energy difference $\Delta\epsilon$ arising from the confinement. A dot is said to have 0D (zero-dimensional) states if $\Delta\epsilon$ is larger than the thermal energy k_BT. Usually, *elastic* tunnel processes through such discrete quantum states are investigated. In the presence of a high-frequency signal *inelastic* transport processes are also possible. Electrons can then reach previously inaccessible energy states by absorbing or emitting photons from the high-frequency signal during tunnelling. This is known as photon-assisted tunnelling (PAT).

The theory of PAT for a single tunnel junction dates back to the work of Tien and Gordon in 1963 [1]. Experiments with high-frequency signals applied to a quantum point contact were reported in [2]. In these experiments, however, PAT could not be demonstrated unambiguously. PAT has been demonstrated in superlattices irradiated by a free electron laser [3]. PAT was also shown in quantum dots without 0D states [4, 5]. Here, we discuss a Tien–Gordon model for quantum dots containing 0D states. We present simulations on the interplay between PAT processes and 0D states. (Such tunnel processes are sketched in the inset of figure 2.) The simulations can be used to study the effects of relaxation processes. Finally, we discuss measurements on PAT through 0D states.

2. PAT through a single junction

Our first step is to look at photon-assisted transport through a single tunnel junction. Suppose that we have an oscillating potential difference across a tunnel junction $\tilde{V}\cos(\omega t)$: in which $\tilde{V}$ is the a.c. amplitude and ω is the angular frequency. This gives a Hamiltonian $H = H_0 + H_{\rm int} = H_0 + e\tilde{V}\cos(\omega t)$. H_0 is the unperturbed Hamiltonian describing the two leads on either side of the tunnel junction. The effect of the oscillating potential is that the time-dependent part of the electron wavefunction, when expanded into a power series, contains the energy components E, $E \pm \hbar\omega$, $E \pm 2\hbar\omega, \ldots$, etc where $\hbar\omega$ is the photon energy. These energy components are called sidebands. The expansion can be done as [1]

$$\begin{aligned}\psi(\boldsymbol{r}, t) &= \varphi(\boldsymbol{r}) \exp\left(-\mathrm{i}\int \mathrm{d}t[E + e\tilde{V}\cos(\omega t)]/\hbar\right) \\ &= \varphi(\boldsymbol{r}) \exp(-\mathrm{i}Et/\hbar) \sum_{n=-\infty}^{\infty} J_n(e\tilde{V}/\hbar\omega) \exp(-\mathrm{i}n\omega t) \\ &= \varphi\left(\sum_{n=-\infty}^{\infty} J_n(e\tilde{V}/\hbar\omega) \exp[-\mathrm{i}(E + n\hbar\omega)t/\hbar]\right) \quad (1)\end{aligned}$$

$\varphi(\boldsymbol{r})$ is the space-dependent part of the wavefunction $\psi(\boldsymbol{r}, t)$. $J_n(\alpha)$ is the nth-order Bessel function of the first kind evaluated at $\alpha = e\tilde{V}/\hbar\omega$. The sidebands are only well defined if the number of tunnel events per unit of time (i.e. the tunnel rates) are much smaller than the photon frequency. Because there is no electric field in the scattering-free leads, mixing of electron states in the leads is absent [6]. The probability for tunnelling from an occupied state E to an unoccupied state $E + n\hbar\omega$ is given by $P(E \rightarrow E + n\hbar\omega) = J_n^2(\alpha)$. A positive (negative) n corresponds to the absorption (emission) of n photons during the tunnel process. Elastic tunnelling without photons corresponds to $n = 0$.

A net current flows by introducing an asymmetry, for instance, by applying a d.c. bias voltage V_0 between the two leads. If tunnelling is a weak perturbation, the current in the presence of microwaves $\tilde{I}$ is given by [1]

$$\begin{aligned}\tilde{I}(V_0) = c \sum_{n=-\infty}^{\infty} & J_n^2(e\tilde{V}/\hbar\omega) \\ & \times \int_{-\infty}^{\infty} [f_1(E - eV_0) - f_r(E + n\hbar\omega)]\rho_A(E - eV_0) \\ & \times \rho_B(E + n\hbar\omega)\,\mathrm{d}E\end{aligned}$$

0268-1242/96/111512+04$19.50

$$= \sum_{n=-\infty}^{\infty} J_n^2(e\tilde{V}/\bar{h}\omega) I(V_0 + n\bar{h}\omega/e). \quad (2)$$

$f(E)$ is the Fermi function, ρ_A and ρ_B are the unperturbed densities of states of the two leads, c is a constant, which is proportional to the tunnel conductance, and I is the tunnel current without an oscillating field. For a *single* junction the d.c. current in the presence of microwaves is thus simply described in terms of the d.c. current without microwaves. Note that for a *double* junction equation (2) is not valid, as will be shown in the following.

3. The 0D model based on a master equation

Our model is based on a master equation approach [7] with the inclusion of PAT. We assume $E_c \gg \Delta\epsilon, k_B T, hf = \bar{h}\omega$ such that we can use a two-state (N and $N+1$) model [8]. We neglect level broadening due to a finite lifetime of the electrons on the dot. A quantum dot state can be described by the total number of electrons on the dot (which is either N or $N+1$) together with χ which describes the particular distribution of electrons over the 0D states. The net current through the dot I follows from the probability $P_{N,\chi}$ that a particular distribution is occupied together with the tunnel rates through one of the barriers:

$$I = \sum_{\chi} \sum_{j=\text{empty}} P_{N,\chi} \Gamma^{\text{in}}_{l,j} - \sum_{\chi'} \sum_{j=\text{full}} P_{N+1,\chi'} \Gamma^{\text{out}}_{l,j} \quad (3)$$

Here $\Gamma^{\text{in (out)}}_{l,j}$ are the rates into or out of 0D state j, through the left barrier:

$$\Gamma^{\text{in}}_{l,j}(\epsilon_j) = \Gamma_l \sum_n J_n^2(\alpha_l) f(\epsilon_j - n\bar{h}\omega + eV_0)$$

$$\Gamma^{\text{out}}_{l,j}(\epsilon_j) = \Gamma_l \sum_n J_n^2(\alpha_l)[1 - f(\epsilon_j - n\bar{h}\omega + eV_0)] \quad (4)$$

where Γ_l is the tunnel rate of the left barrier determined by the barrier shape, and ϵ_j is the energy of 0D state j measured relative to the Fermi energy of the right lead. An equivalent set of equations can be given for the right barrier taking $V_0 = 0$. In the following simulations we take equal a.c. amplitudes dropping across the left and right barriers; i.e. $\alpha_l = \alpha_r = \alpha$. The probabilities $P_{N,\chi}$, are calculated from the set of master equations given by

$$\begin{aligned}\dot{P}_{N,\chi} = &\sum_{\chi'} P_{N+1,\chi}(\Gamma^{\text{out}}_{l,j_{\chi'}} + \Gamma^{\text{out}}_{r,j_{\chi'}}) \\ &- P_{N,\chi} \sum_{j=\text{empty}} (\Gamma^{\text{in}}_{l,j} + \Gamma^{\text{in}}_{r,j}) + \sum_{\chi'' \neq \chi} P_{N,\chi''} \Gamma_{\chi'' \to \chi} \\ &- P_{N,\chi} \sum_{\chi''' \neq \chi} \Gamma_{\chi \to \chi'''} \end{aligned} \quad (5)$$

and its equivalent for $\dot{P}_{N+1,\chi'}$. Note that for $N = 2$ we have ten different χ if we include five different 0D states, so we have ten equations $\dot{P}_{N,\chi}$, and another ten equations $\dot{P}_{N+1,\chi'}$. The first two terms in equation (5) correspond to a change in the occupation probability of a certain distribution due to tunnelling (the number of electrons on the dots changes). The first term takes into account the rates that correspond to an electron tunnelling out of state $j_{\chi'}$ leaving the dot in the distribution (N, χ). For an electron tunnelling into the dot one needs to sum over all the states j that are empty when the dot is in state χ (second term). In the last two terms the number of electrons on the dot stays the same, only the distribution over the states changes (i.e. electrons relax to a lower level or they are excited to a higher level). We take excitation rates equal to zero (no mixing of electron states in the dot due to the high frequency) and non-zero relaxation rates.

To find a stationary solution for the occupation probabilities in the dot these equations are set to zero and solved with the boundary condition:

$$\sum_{\chi} P_{N,\chi} + \sum_{\chi'} P_{N+1,\chi'} = 1.$$

The current is calculated for a fixed set of 0D energies $\{\epsilon_j\}$. The effect of a gate voltage is simulated by shifting the 0D energies ϵ_j relative to the Fermi energy of the right reservoir.

Figure 1 shows simulations without relaxation between the states in the dot. We have taken $\Delta\epsilon = 3\bar{h}\omega$ for the curves in the inset. Next to the main resonance we see that side peaks develop at multiple values of $\bar{h}\omega/e$ when α is increased. In the main figure we have taken $\Delta\epsilon = 0.75\bar{h}\omega$. Here not only do side peaks develop but we also see peaks at other gate voltages. These peaks arise due to the interplay between the 0D states and the photon energy. Their locations are described by $(m\,\Delta\epsilon + n\bar{h}\omega)/e$ where $m = 0, \pm 1, \pm 2, \ldots$ and n is the photon number. Similar simulation results have been reported by Bruder and Schoeller [9].

Figure 2 shows an expansion for the curve $\alpha = 1$. We have assigned the excited states ϵ_j and the particular PAT process. The $N+1$ ground state is denoted by $j = 0$, positive j are excited states above ϵ_0 and negative j are below ϵ_0. Note that a curve like this resembles an atomic spectrum. The inset shows the effects of relaxation. It is seen that upon increasing the relaxation rate the peaks that correspond to transitions through excited states decrease while the peaks corresponding to transitions through the ground state increase.

4. Experiments

In figure 3 data are shown from a dot with a measured 0D splitting of approximately 140 μeV. This is four or five times larger than the thermal energy. With a split gate technique a small dot of lithographic size 600×300 nm^2 was formed in the 2DEG of a GaAs/AlGaAs heterostructure with mobility 2.3×10^6 cm^2 V^{-1} s^{-1} and electron density 1.9×10^{15} m^{-2} at 4.2 K. In addition to the d.c. voltages on the gates a microwave signal (0–75 GHz) was capacitatively coupled to one of the gates. The effective electron temperature was found to be about 300 mK. The charging energy $E_c = 1.2 \pm 0.1$ meV. Using finite bias voltage measurements the energy splitting between the ground state and the first excited state was determined to be approximately 140 μeV (four or five times larger than the thermal energy) and the conversion factor from gate voltage to energy could be deduced.

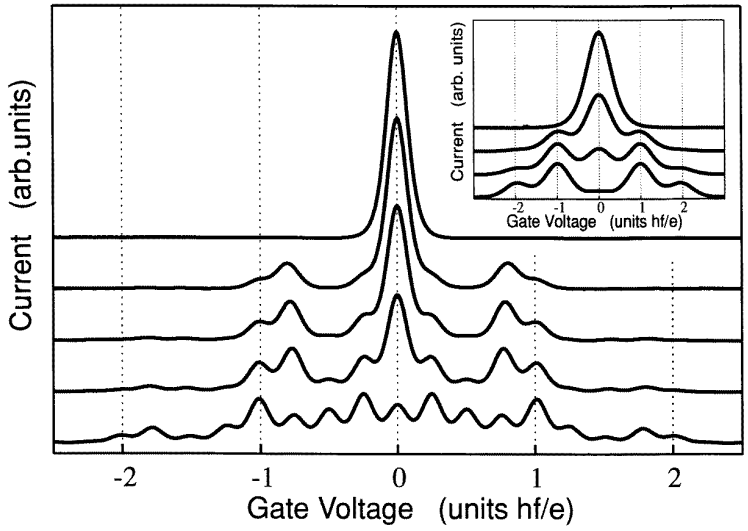

Figure 1. Simulation without relaxation. The parameters for the data in the inset are $\Delta\epsilon = 3\hbar\omega$, $hf = 5k_BT$, and from top to bottom $\alpha = 0, 1, 1.5, 2$. The parameters for the main figure are $\Delta\epsilon = 0.75\hbar\omega$, $hf = 20k_BT$ and from top to bottom $\alpha = 0, 0.5, 0.75, 1, 1.5$.

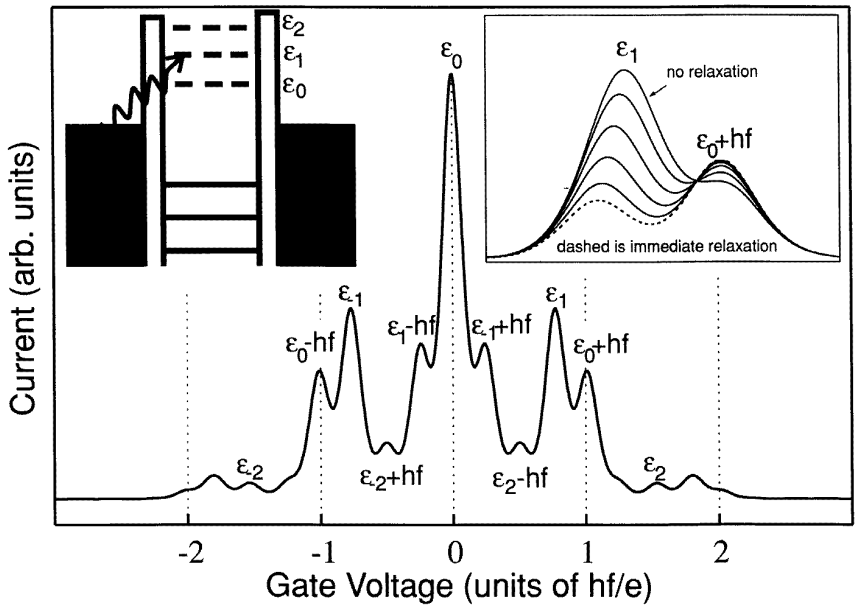

Figure 2. Expansion for the curve $\alpha = 1$ from figure 1. The right inset shows the effects of increasing relaxation. The relaxation rates divided by the tunnel rate are 0, 0.1, 0.35, 1, 3.5 and infinite. The left inset sketches a photon absorption process to overcome the Coulomb gap.

The d.c. current I was measured as a function of the d.c. gate voltage V_g in the presence of a microwave signal. The data shown in figure 3 were taken at 45 GHz for different microwave powers corresponding to α ranging from 1 to 3. The photon energy $hf = 185$ μeV is indicated by the vertical dotted lines in the figure. Bumps with a spacing corresponding to the photon energy are clearly seen. We interpret these bumps as photon side peaks. Additional structure due to excited 0D states in between photon side peaks is washed out, probably because the difference between the photon energy and the 0D splitting is comparable to temperature. At higher powers the neighbouring Coulomb peak starts to lift the current at the right of the peak.

The broken curves are fits. The lower curve has $\alpha = 1$ and no relaxation. The upper curve fitted best with $\alpha = 1.4$ and 50% relaxation. However, it is not clear whether the incorporation of relaxation is really required to explain the data.

Our measurements do show for the first time PAT through discrete 0D states. With a lower electron temperature the side peaks should become more pronounced

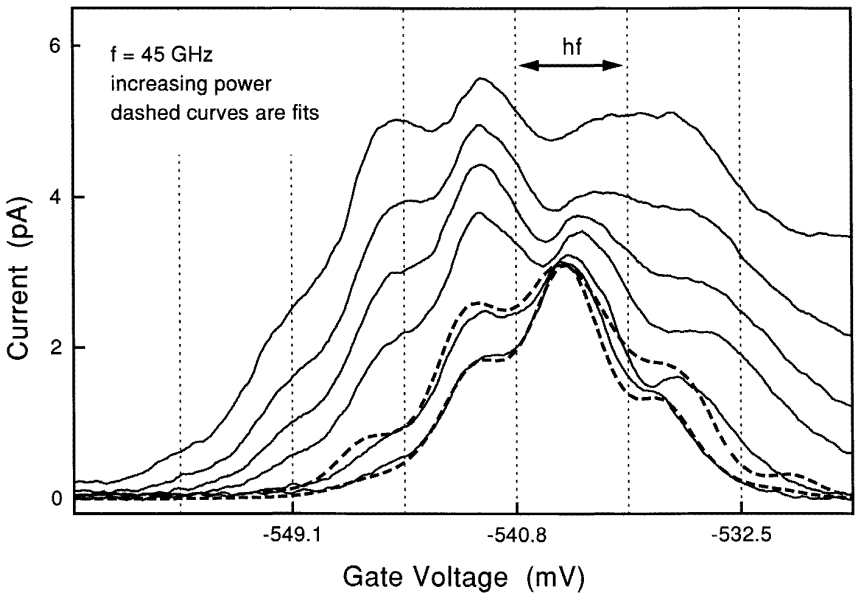

Figure 3. A measurement of a single Coulomb peak in the presence of microwaves with f = 45 GHz. The different curves are for increasing power. The two broken curves are fits for α = 1 and 1.4.

and a more detailed comparison between simulations and experiments may give information concerning relaxation processes. Future work will also include PAT in double dots with zero-dimensional states. Here it should be possible to attain a higher resolution [10]. Double dots are also promising for studying coherent tunnel processes involving PAT [11].

Acknowledgments

We would like to thank P Lukey, S F Godijn and J E Mooij for discussions and experimental help. Also we thank Philips Laboratories and C T Foxon for providing the heterostructures. LPK was supported by the Royal Netherlands Academy of Arts and Sciences.

References

[1] Tien P K and Gordon J R 1963 *Phys. Rev.* **129** 647
[2] Patel N K *et al* 1991 *Proc. 20th Int. Conf. on the Physics of Semiconductors* ed E M Anastassakis and J D Joannopoulos (Singapore: Scientific) p 2371
Wyss R A *et al* 1993 *Appl. Phys. Lett.* **63** 1522; 1995 *Appl. Phys. Lett.* **66** 1144
Jansen T J B M *et al* 1994 *J. Phys.: Condens. Matter* **6** L163
[3] Guimarães P S S *et al* 1993 *Phys. Rev. Lett.* **70** 3792
Keay B J *et al* 1995 *Phys. Rev. Lett.* **75** 4098; 1995 *Phys. Rev. Lett.* **75** 4102
[4] Kouwenhoven L P *et al* 1994 *Phys. Rev.* B **50** 2019; 1994 *Phys. Rev. Lett.* **73** 3443
[5] Blick R H *et al* 1995 *Appl. Phys. Lett.* **67** 3924
[6] Mixing is described by J Iñarrea, G Platero and C Tejedor 1994 *Phys. Rev.* B **50** 4581
[7] Averin D V *et al* 1991 *Phys. Rev.* B **44** 6199
Beenakker C W J 1991 *Phys. Rev.* B **44** 1646
[8] Wan J C *et al* 1991 *Phys. Rev.* B **43** 9381
[9] Bruder C and Schoeller H 1994 *Phys. Rev. Lett.* **72** 1076
[10] van der Vaart N C *et al* 1995 *Phys. Rev. Lett.* **74** 4702
[11] Stoof T H and Nazarov Yu V 1995 *Phys. Rev.* B **51**
Stafford C A and Wingreen N S 1996 *Phys. Rev. Lett.* **76** 1916